Eur. Phys. J. A **25**, 49–55 (2005)
DOI 10.1140/epja/i2005-10075-5

THE EUROPEAN PHYSICAL JOURNAL A

# Shears band with a large dynamic moment of inertia in $^{197}$Bi

G.K. Mabala[1,2,a], E. Gueorguieva[1,b], J.F. Sharpey-Schafer[1], M. Benatar[1,2], R.W. Fearick[2], K.I. Korir[3], J.J. Lawrie[1], S.M. Mullins[1], S.H.T. Murray[1,2], N.J. Ncapayi[1], R.T. Newman[1], D.G. Roux[1,2,c], F.D. Smit[1], and R. Wyss[4]

[1] iThemba Laboratory for Accelerator Based Sciences, P.O. Box 722, 7129 Somerset West, South Africa
[2] Department of Physics, University of Cape Town, Private Bag, 7701, Rondebosch, South Africa
[3] Schonland Research Centre for Nuclear Sciences, PO WITS 2050, Johanesburg, South Africa
[4] KTH, Royal Institute of Technology, 100 44 Stockholm, Sweden

Received: 24 March 2005 / Revised version: 18 May 2005 /
Published online: 20 June 2005 – 
Communicated by R. Krücken

**Abstract.** High-spin states in $^{197}$Bi were studied with the AFRODITE $\gamma$-ray array at iThemba LABS using the $^{181}$Ta($^{22}$Ne, $6n$) reaction at a beam energy of 125 MeV. A new shears band was found and linked to the low-lying states in $^{197}$Bi. Its dynamic moment of inertia, $\Im^{(2)}$, is considerably larger than the $\Im^{(2)}$ of the shears bands in the neighbouring Pb isotopes. This is probably a result of the involvement of an additional high-$K$ $h_{9/2}$ proton orbital.

**PACS.** 29.30.Kv X- and $\gamma$-ray spectroscopy – 23.20.Lv $\gamma$ transitions and level energies – 21.60.Ev Collective models – 27.80.+w $190 \leq A \leq 219$

## 1 Introduction

During the last couple of decades a number of bands consisting of long regular sequences of $M1$ transitions with weak or missing $E2$ crossovers were discovered in many nuclei which are believed to be spherical [1]. In the $A \sim 200$ mass region such bands were found in several Pb and Bi isotopes [2–13], and also in $^{190}$Hg [14], and were assigned to configurations involving high-$K$ proton particles and low-$K$ neutron holes. These bands were successfully interpreted with the tilted-axis cranking (TAC) model [15, 16] as a result of a rotation around the total-angular-momentum vector that is tilted with respect to the principal axes of the nucleus. Since the perpendicular component of the magnetic moment vector rotates around the total angular momentum, this type of rotation is called magnetic. According to this model the spin in the bands is generated by the gradual alignment of the angular momenta of protons and neutrons along the total-angular-momentum axis (shears mechanism) [9], while the rotation of the slightly deformed oblate core is small. It was found that a semiclassical description [17,18] of the alignment of the proton and neutron angular momenta described the experimental data quite well, and a study of the competition between the shears mechanism and the rotation of the oblate core suggested that the shears mechanism dominates only at low deformations with $\varepsilon_2 \leq 0.12$ [19].

Recently, the quadrupole deformation of the $11^-$ isomeric states built on the proton $\pi[i_{13/2}h_{9/2}]_{K=11}$ configuration common to many of the shears bands in the Pb region, was measured as $\beta_2 = 0.21(4)$ in $^{194}$Pb, [20] and $\beta_2 = 0.156(28)$ in $^{196}$Pb, [21]. It should be noted that the deformation corresponding to the shears bands is essentially determined by the polarization effects of the excited protons across the $Z = 82$ shell gap [22]. TAC calculations also suggested that the deformation of the shears bands is similar to that of the relevant high-$K$ proton state [21]. Thus, nuclear deformations larger than $\varepsilon_2 = 0.10$–$0.12$, (values usually used with the TAC model), might be associated with some shears bands in this mass region. On the other hand, the preliminary results on the quadrupole deformation for the $11^-$ isomer in $^{192}$Pb and for the shears bandhead level $29/2^-$ in $^{193}$Pb show smaller values of $\varepsilon_2 = 0.11(2)$ [22] and $\varepsilon_2 = 0.12$ [22,23]. Thus, it seems interesting to investigate more shears bands in this mass region and to establish the trend of the nuclear deformation of these states, since this is strongly related to the competition between the shears mechanism and the rotation of the oblate core.

In this work, high-spin states in $^{197}$Bi were investigated in order to search for shears bands. Previous studies have

[a] *Present address*: NECSA, P.O. Box 582, Pretoria, South Africa; e-mail: mabala@tlabs.ac.za
[b] e-mail: elena@tlabs.ac.za
[c] *Present address*: University of Western Cape, Private Bag X17, 7535 Bellville, South Africa.

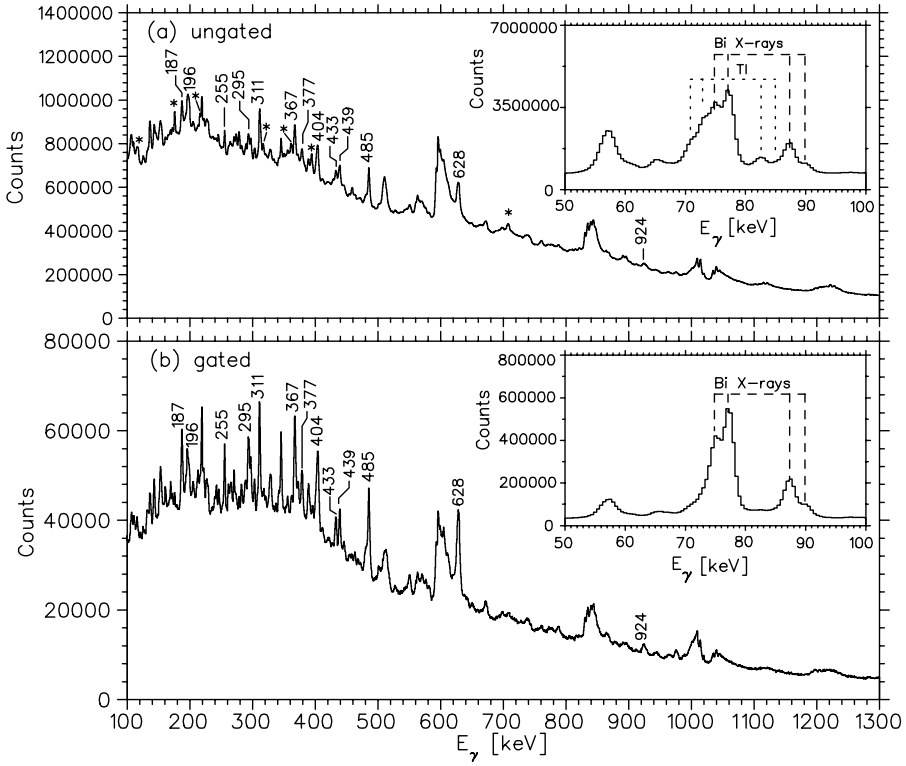


**Fig. 1.** The total projection spectra extracted from the (a) ungated and (b) gated on the $K_\alpha$ X-rays of Bi, $\gamma$-$\gamma$ matrices. The transitions from $^{195}$Tl are marked with stars. The low-energy parts of the spectra are shown in the inserts.

established the level scheme of $^{197}$Bi only up to an excitation energy of $\sim$ 4 MeV [24,25].

## 2 Experimental details

The $^{197}$Bi nuclei were populated using the $^{181}$Ta($^{22}$Ne, $6n$) reaction at a beam energy of 125 MeV. The beam was provided by the $K = 200$ Separated Sector Cyclotron at the iThemba Laboratory for Accelerator Based Sciences, near Cape Town. The beam current was $\sim$ 10 nA with a beam-burst separation of 66 ns. The target was a thin self-supporting 333 $\mu$g/cm$^2$ foil of $^{181}$Ta (99.988%). $\gamma$-rays were detected with the AFRODITE array [26], which is comprised of 8 segmented low-energy photon spectrometers (LEPS) and seven Compton-suppressed clover detectors arranged in three rings at 45°, 90°, and 135° with respect to the beam direction. The trigger logic was set to accept events when at least three of the fifteen detectors had fired in coincidence and $\sim 528 \times 10^6$ coincidence events were recorded in total. The presence of a number of long-lived isomeric states in $^{197}$Bi, and the use of a thin target made the measurement of the relative strength of the exit channels in this reaction impossible. According to PACE2 [27,28] calculations, fission takes place in 72% of the cases, while the yield of the major fusion-evaporation product, $^{197}$Bi, is $\sim$ 12%. The large component of fission products in this reaction made several parts of the data analysis very difficult. Furthermore, a relatively large yield of $^{195}$Tl was populated through incomplete fusion, which further complicated the analysis. A substantial selectivity was obtained by gating on the $K_{\alpha1}$ (77 keV) and $K_{\alpha2}$ (75 keV) X-rays of Bi.

The event data were energy and efficiency calibrated using $^{152}$Eu and $^{133}$Ba sources and corrected for Doppler shifts corresponding to the measured recoil velocity $v/c = 0.010(4)$. Clover data were sorted into ungated and gated (on the Bi $K_\alpha$ X-rays detected by the LEPS detectors) $E_\gamma$-$E_\gamma$ matrices, and the $\gamma$-ray coincidences were studied using RadWare software [29]. The total projection spectrum obtained from the ungated matrix is plotted in fig. 1(a), while the total projection spectrum extracted from the gated matrix is shown in fig. 1(b). The large background produced from fission products and also the contribution from the $^{195}$Tl transitions were considerably reduced by gating on the Bi $K_\alpha$ X-rays. Such gated spectra were extensively used for establishing the $\gamma$-$\gamma$ coincidences in $^{197}$Bi.

In order to determine the multipole order of the $\gamma$-ray transitions, Directional Correlation of Decays from Oriented nuclear states (DCO) [30] was performed. Two $E_\gamma$-$E_\gamma$ matrices were constructed from the clover data, the first (symmetric) matrix contained only coincidence events for which both $\gamma$-rays were detected at 45° or 135°. The second (asymmetric) matrix contained the coincidences between $\gamma$-rays detected at 45° or 135° (placed on the $y$-axis) and $\gamma$-rays detected at 90° (placed on the $x$-axis). The same gates were applied on the $y$-axes of both matrices and the DCO ratios for a given $\gamma$-ray was obtained as the ratio, $R_{\rm DCO} = A_\gamma(45°, 135°)/A_\gamma(90°)$, of

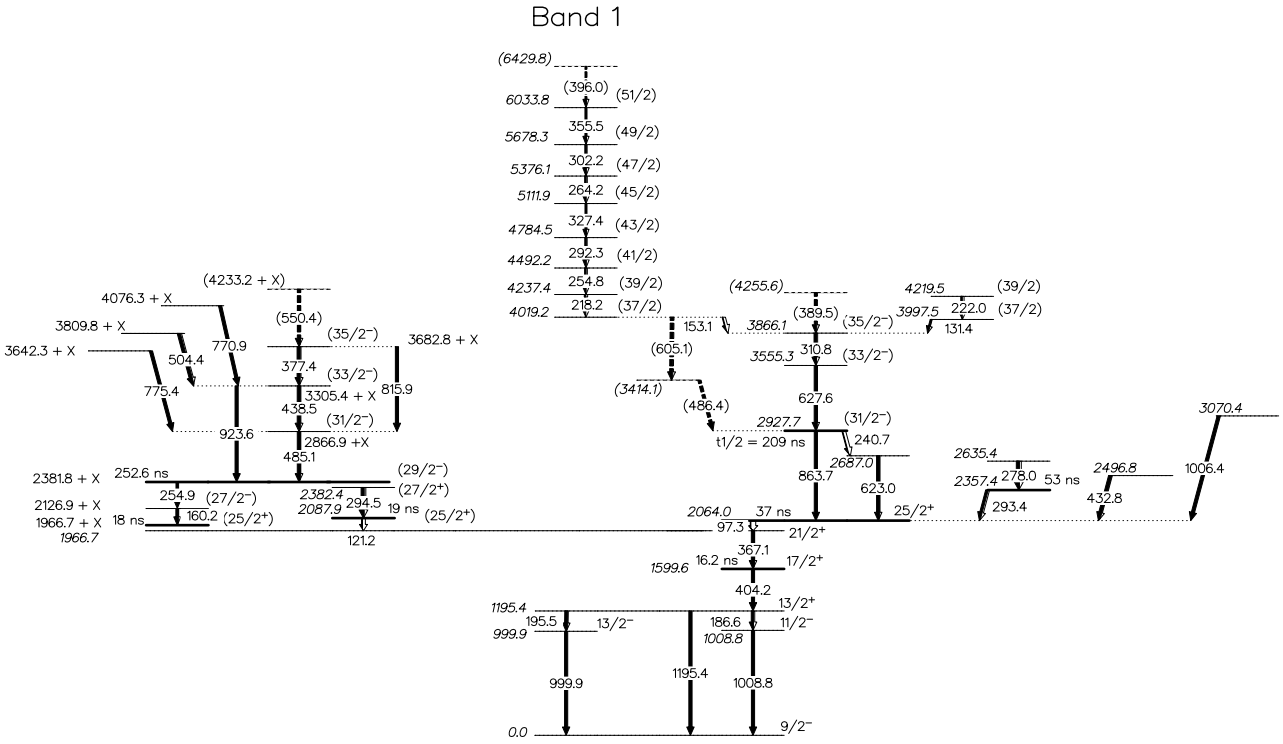


**Fig. 2.** The level scheme of $^{197}$Bi deduced from the present work.

the corresponding peak areas in the two gated spectra. The average $R_{\rm DCO}$ ratios for the known stretched dipole transitions were found to be $\sim 0.7$, while the average values for the known stretched quadrupole transitions were $\sim 1.2$. In order to determine the parities of the $\gamma$-ray transitions, linear polarization measurements were performed with the clover detectors that were placed at 90° with respect to the beam direction. The polarization asymmetry, $A_{\rm pol}$, for a given $\gamma$-ray was measured as $A_{\rm pol} = (A_{\rm V} - \alpha A_{\rm H})/(A_{\rm V} + \alpha A_{\rm H})$, where the $A_{\rm V}$ ($A_{\rm H}$) denotes the area of the corresponding peak in the spectrum containing only vertically (horizontally) Compton-scattered events in a clover, and $\alpha$ is the relative efficiency, measured as $\alpha = 1.05$. The recoil shadow anisotropy method (RSAM) [31] was employed to search for isomeric states with lifetimes in the nanosecond range, but no evidence for new isomeric states in $^{197}$Bi was found.

## 3 Results

The known level scheme of $^{197}$Bi [24,25] is extended to higher spins and a new dipole band consisting of $M1$ transitions is found, as shown in fig. 2. $\gamma$-$\gamma$ coincidence, DCO ratios, linear polarization and $\gamma$ intensity measurements were performed and the values obtained, together with the spin and energy assignments of the transitions in $^{197}$Bi, are summarized in table 1.

Our data were not well suited for studying the transitions lying at low excitation energy in $^{197}$Bi. Due to several long-lived isomeric states and the use of a thin target, these transitions were emitted away from the focal centre of the array, and thus have reduced intensities in the data. The observed coincidence relationships for these transitions in our data were consistent with those previously suggested in the $^{197}$Bi level scheme [24,25], and in particular they confirm the anticoincidence of the 97.3 and 294.5 keV transitions as reported in ref. [25].

Several new transitions were placed above the $(29/2^-)$ isomeric level at $2381.8 + x$ keV according to their coincidences with the 485.1 and 438.5 keV transitions and their mutual coincidences. The spectrum gated on the 550 keV transition shows a self-coincidence and thus indicates the existence of another 550 keV transition in $^{197}$Bi, which is not yet placed in the level scheme. A spectrum, double gated on the 485 keV transition and the $K_\alpha$ X-rays of Bi, showing the new transitions above the $(29/2^-)$ isomeric level is plotted in fig. 3(a).

All the transitions above the $(31/2^-)$ isomeric level at 2927.7 keV are new, apart from the 627.6 and 310.8 keV transitions. The previously suggested 863.7 and 240.7 keV transitions de-exciting this isomeric level could not be observed in our data, probably because they are delayed and thus are emitted further from the centre of the array. Stretched magnetic character was suggested for the 627.6 and 310.8 keV transitions by the DCO and linear polarization measurements. A spectrum double gated on the 310.8 keV transition and the $K_\alpha$ X-rays of Bi is shown in fig. 3(b).

The new transitions that constitute Band 1 were found in mutual coincidence and in coincidence with the 310.8 and 627.6 keV transitions. A spectrum double gated on the

**Table 1.** Energy, intensity, DCO ratios, linear polarization asymmetry of the transitions in $^{197}$Bi. The spin assignments and the energies of the initial levels are also included.

| $E_\gamma$ (keV) | $I_\gamma^{(a)}$ | $R_{\rm DCO}$ | $A_{\rm pol}$ | $E_{\rm in}$ (keV) | $I_{\rm i}^\pi \rightarrow I_{\rm f}^\pi$ |
|---|---|---|---|---|---|
| 97.3 | | 1.24(28) | | 2064.0 | $25/2^+ \rightarrow 21/2^+$ |
| 121.2 | | | | 2087.9 | $(25/2^+) \rightarrow 21/2^+$ |
| 131.4 | | 0.55(25) | | 3997.5 | $(37/2) \rightarrow (35/2^-)$ |
| 153.1 | 12(6) | 0.56(22) | | 4019.2 | $(37/2) \rightarrow (35/2^-)$ |
| 160.2 | | 0.77(16) | | $2126.9 + x$ | $(27/2^-) \rightarrow (25/2^+)$ |
| 186.6 | | 0.74(8) | | 1195.4 | $13/2^+ \rightarrow 11/2^-$ |
| 195.5 | | 0.70(14) | | 1195.4 | $13/2^+ \rightarrow 13/2^-$ |
| 222.0 | | 0.66(14) | | 4219.5 | $(39/2) \rightarrow (37/2)$ |
| 240.7 | | | | 2927.7 | $(31/2^-) \rightarrow$ |
| 254.9 | | | | $2381.8 + x$ | $(29/2^-) \rightarrow (27/2^-)$ |
| 278.0 | | | | 2635.4 | |
| 293.4 | | 0.55(9) | | 2357.4 | $\rightarrow 25/2^+$ |
| 294.5 | | 0.63(10) | | 2382.4 | $(27/2^+) \rightarrow (25/2^+)$ |
| 310.8 | 40(12) | 0.49(10) | −0.06(1) | 3866.1 | $(35/2^-) \rightarrow (33/2^-)$ |
| 367.1 | | 0.88(7) | +0.06(1) | 1966.7 | $21/2^+ \rightarrow 17/2^+$ |
| 377.4 | | 0.55(14) | | $3682.8 + x$ | $(35/2^-) \rightarrow (33/2^-)$ |
| (389.5) | | 0.58(12) | | (4255.6) | $\rightarrow (35/2^-)$ |
| 404.2 | | 1.17(9) | | 1599.6 | $17/2^+ \rightarrow 13/2^+$ |
| 432.8 | | 0.65(15) | | 2496.8 | $\rightarrow 25/2^+$ |
| 438.5 | | 0.54(14) | −0.02(1) | $3305.4 + x$ | $(33/2^-) \rightarrow (31/2^-)$ |
| 485.1 | | 0.54(9)$^{(b)}$ | −0.04(4) | $2866.9 + x$ | $(31/2^-) \rightarrow (29/2^-)$ |
| (486.4) | | 0.54(9)$^{(b)}$ | | 3414.1 | $\rightarrow (31/2^-)$ |
| 504.4 | | | | $3809.8 + x$ | $\rightarrow (33/2^-)$ |
| (550.0) | | 0.64(18) | | $(4233.2 + x)$ | $\rightarrow (35/2^-)$ |
| (605.1) | | | | 4019.2 | $(37/2) \rightarrow$ |
| 623.0 | | | | 2687.0 | $\rightarrow 25/2^+$ |
| 627.6 | | 0.54(7) | −0.03(1) | 3555.3 | $(33/2^-) \rightarrow (31/2^-)$ |
| 770.9 | | | | $4076.3 + x$ | $\rightarrow (33/2^-)$ |
| 775.4 | | | | $3642.3 + x$ | $\rightarrow 31/2^-$ |
| 815.9 | | | | $3682.8 + x$ | $(35/2^-) \rightarrow (31/2^-)$ |
| 863.7 | | | | 2927.7 | $(31/2^-) \rightarrow 25/2^+$ |
| 923.6 | | 1.11(25) | +0.06(2) | $3305.4 + x$ | $(33/2^-) \rightarrow (29/2^-)$ |
| 999.9 | | | | 999.9 | $13/2^- \rightarrow 9/2^-$ |
| 1006.4 | | | | 3070.4 | $\rightarrow 25/2^+$ |
| 1008.8 | | | | 1008.8 | $11/2^- \rightarrow 9/2^-$ |
| 1095.4 | | | | 1095.4 | $13/2^+ \rightarrow 9/2^-$ |
| *Band* 1 | | | | | |
| 218.2 | 26(8) | 0.54(6) | | 4237.4 | $(39/2) \rightarrow (37/2)$ |
| 254.8 | 20(8) | 0.64(7) | | 4492.2 | $(41/2) \rightarrow (39/2)$ |
| 264.2 | 7(4) | 0.46(18) | | 5376.1 | $(47/2) \rightarrow (45/2)$ |
| 292.3 | 18(8) | 0.59(9) | | 4784.5 | $(43/2) \rightarrow (41/2)$ |
| 302.2 | 6(4) | 0.52(16) | | 5678.3 | $(49/2) \rightarrow (47/2)$ |
| 327.4 | 14(6) | 0.47(17) | −0.05(2) | 5111.9 | $(45/2) \rightarrow (43/2)$ |
| 355.5 | 5(4) | 0.49(23) | | 6033.8 | $(51/2) \rightarrow (49/2)$ |
| (396.0) | | | | 6429.8 | $\rightarrow (51/2)$ |

(a) The intensities are normalized with respect to the intensity of the 311 keV transition.
(b) Non-separated doublet. The value corresponds to the total peak.

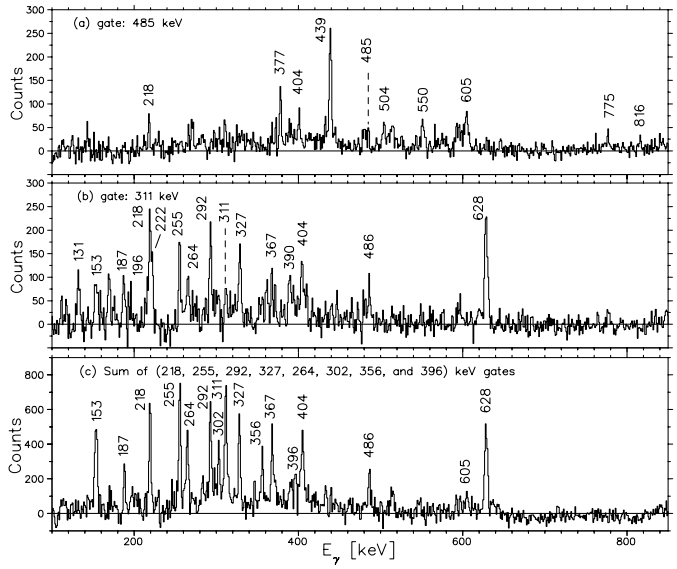


**Fig. 3.** Spectra extracted from the matrix gated on the $K_\alpha$ Bi X-rays and also gated on the: (a) 485 keV transition, showing the new transitions above the $(29/2^-)$ isomer, (b) 311 keV transition, showing the new transitions above the $(31/2^-)$ isomer, and (c) transitions of Band 1.

Bi $K_\alpha$ X-rays and on the transitions from Band 1 is shown in fig. 3(c). The DCO measurements showed stretched dipole character for these transitions. Among the transitions of the band, the polarization asymmetry could be measured only for the 327.4 keV $\gamma$-ray and showed magnetic nature. No crossover transitions belonging to this band were observed. Where possible, the transitions were ordered according to their intensity. The topmost transitions, (356, 302, and 264 keV), may have a different ordering.

Band 1 decays to the lower-lying states in $^{197}$Bi through the 153.1 and the tentative 605.1 keV transitions. The 153 keV peak is quite wide in the gated spectra, suggesting that another as yet unplaced transition with a similar energy belongs to this nucleus.

A spin of (37/2) is suggested for the 4019.2 keV level of Band 1, based on the previous tentative assignment of $I^\pi = (31/2^-)$ to the 2927.7 keV isomeric level [24] and the stretched dipole character of the 627.6, 310.8 and 153.1 keV transitions. It was difficult to deduce the electric or magnetic nature of the 153.1 keV transition from its intensity (when gating on the transitions of the band, the total intensity of this transition should be similar to the total intensity of the 310.8 and 627.6 keV transitions), because of contaminated gating transitions and also because the 153 keV transition seems to be a doublet in $^{197}$Bi. However, although the measured intensity did not allow us to unambiguously deduce the nature of this $\gamma$-ray, it indicates that a magnetic character is more likely and thus favours a negative parity for Band 1.

## 4 Discussion

A number of dipole bands found in the Pb-Bi region were associated with magnetic rotation [2–12,14], and assigned to configurations involving high-$K$ proton particles and low-$K$ neutron holes. Thus, it is likely that Band 1 in $^{197}$Bi is also built on a high-$K$ proton and low-$K$ neutron states. Its excitation energy ($\sim 4$ MeV) is consistent with a four-quasiparticle excitation, and thus it is suggested that Band 1 involves a three-proton–two-neutron configuration. The proton configurations assigned to the most intense shears bands in the Pb isotopes involve the two high-$K$ $h_{9/2}[505]9/2^-$ and $i_{13/2}[606]13/2^+$ proton orbitals. In the heavier $^{198-202}$Bi nuclei, the observed shears bands were associated with the same two $h_{9/2}$ and $i_{13/2}$ proton orbitals, while the third proton was assigned to a $s_{1/2}$ orbital because the dynamic moments of inertia, $\Im^{(2)}$, of the bands in the Bi isotopes were found to be similar to those of the shears bands in the Pb nuclei [12,13].

In the top panel of fig. 4 the spin, $I$, of Band 1 in $^{197}$Bi is shown as a function of the $\gamma$-ray energy, $E_\gamma$, together with the data for the two most intense bands in the $^{196}$Pb isotone [7] with configurations $\pi h_{9/2}i_{13/2} \otimes \nu i^2_{13/2}$ and $\pi h_{9/2}i_{13/2} \otimes \nu i_{13/2}\nu j$, ($j = p_{3/2}$, $f_{5/2}$). The increase in the spin for Band 1 in $^{197}$Bi seems to be much faster than for the two bands in $^{196}$Pb, indicating a larger dynamic moment of inertia. The large difference in the values of the $\Im^{(2)}$'s of these bands can be seen in the bottom panel of fig. 4, where the $\Im^{(2)}$'s for the three bands at frequencies below the first band crossing are plotted. Moreover, the $\Im^{(2)}$ of Band 1 in $^{197}$Bi is compared with the $\Im^{(2)}$'s of the two most intense shears bands in the even-even Pb isotopes [3,5,7,8] and also with the $\Im^{(2)}$'s of the known shears bands in the odd Bi nuclei [12] (see fig. 5). Considerably larger values of $\Im^{(2)}$ are found for Band 1 in $^{197}$Bi and Band 2 in $^{199}$Bi [12]. It should be noted that above the first band crossing the values of $\Im^{(2)}$ in the shears bands in the Pb isotopes become somewhat larger as a result of the excitation of a second neutron pair and, thus, a decrease in the pairing strength. However, it seems unlikely that the large $\Im^{(2)}$ in $^{197}$Bi is due to the involvement of an additional neutron pair, since a higher spin and excitation energy would be necessary. It thus seems plausible to suggest that the larger values of $\Im^{(2)}$ in $^{197}$Bi are a result of a different configuration, *i.e.* a result of the involvement of an additional intruder orbital. Thus, a configuration of three high-$K$ protons, $\pi[i_{13/2}h^2_{9/2}]_{K=14.5}$ is proposed. Due to the higher dynamic moment of inertia of the band in $^{199}$Bi, it may also be built on a three high-$K$ proton configuration (contrary to the previously suggested $\pi i_{13/2}h_{9/2}s_{1/2}$ configuration [12]).

The most intense shears bands in the Pb nuclei were assigned to neutron configurations such as $\nu i^2_{13/2}$ and $\nu i_{13/2}\nu j$, where $j = (p_{3/2}, f_{5/2})$. The latter corresponds to the yrast shears band in the $^{196}$Pb isotone, and, thus, it is a likely candidate for Band 1 in $^{197}$Bi. The suggested spin of (37/2) for the 4019.2 keV level and the likely negative parity of the band are consistent with this assignment. Assuming an angular momentum of $\sim 7\hbar$ for this neutron

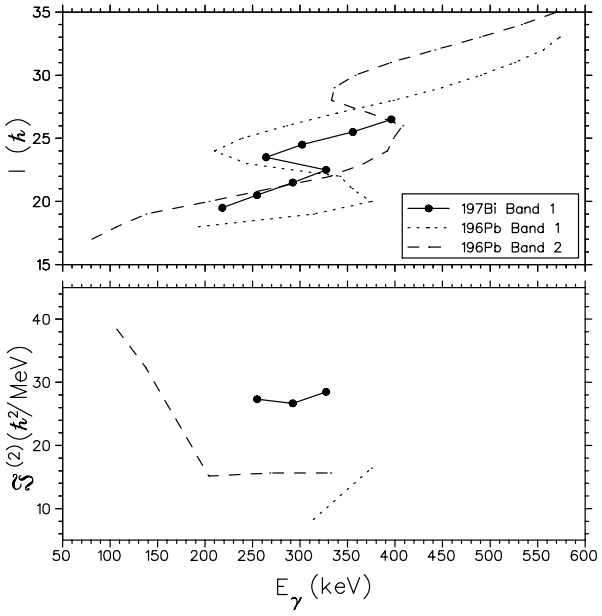


**Fig. 4.** The spin (top panel) and the dynamic moment of inertia $\Im^{(2)}$ (bottom panel), as a function of the transition energy for Band 1 in $^{197}$Bi and for the two most intense bands in the $^{196}$Pb isotone. $\Im^{(2)}$ values are plotted for transitions below the corresponding first band crossings. The data for $^{196}$Pb is from ref. [7].

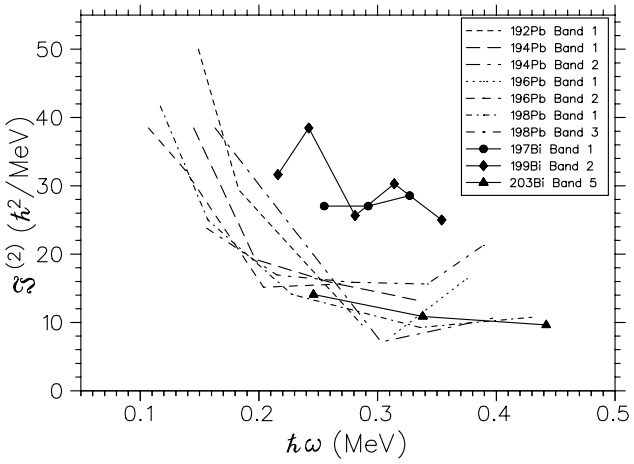


**Fig. 5.** The dynamic moments of inertia $\Im^{(2)}$ of Band 1 in $^{197}$Bi and of the two most intense bands in the even-even $^{192-198}$Pb isotopes, as well as the $\Im^{(2)}$ of the known bands in the odd Bi nuclei. $\Im^{(2)}$'s for transitions below the corresponding first band crossings are plotted.

configuration and a perpendicular coupling to the three high-$K$ protons, a bandhead level $I^\pi \sim 33/2^-$ results. However, the other possible neutron configuration, *i.e.* $\nu i^2_{13/2}$, (corresponding to a bandhead level $I^\pi \sim 37/2^+$) may not be ruled out.

An irregularity in the smooth increase of the spin is found in $^{197}$Bi at a transition energy of about 300 keV (see the top panel of fig. 4). It corresponds to a much smaller gain in the alignment than the one observed in the two

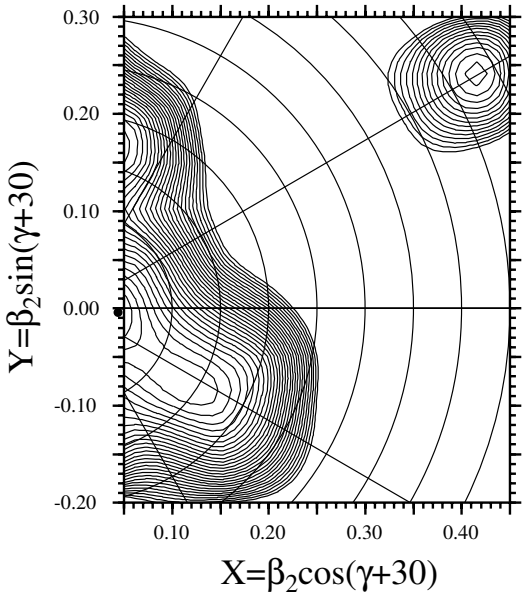


**Fig. 6.** TRS calculation for the $(\pi, \alpha) = (+, +1/2)$ configuration in $^{197}$Bi at $\hbar\omega = 0.282$ MeV.

**Table 2.** TRS calculations for the $(\pi, \alpha) = (+, +1/2)$ configuration in $^{197}$Bi at $\hbar\omega = 0.282$ MeV.

| $I_p$ | $I_n$ | $\beta_2$ | $\gamma$ | Shape |
|---|---|---|---|---|
| 5.7 | 12.6 | 0.04 | $-36°$ | spherical |
| 1.6 | 15.8 | 0.14 | $-64°$ | oblate collective |
| 14.0 | 2.1 | 0.17 | $> 44°$ | oblate non-collective |
| 12.1 | 19.4 | 0.48 | $0°$ | superdeformed |

bands of the $^{196}$Pb isotone, which in Pb corresponds to the excitation of a second neutron pair. However, since the ordering of the topmost transitions in Band 1 in $^{197}$Bi is uncertain, further studies are needed in order to understand the nature of this irregularity.

The $M1$ bands observed in the Pb-Bi region are believed to be shears bands generated by magnetic rotation. Thus, the proton particle and the neutron hole angular momenta, initially coupled perpendicularly to each other, align towards the direction of the total angular momentum (shears mechanism), and generate the spin in the band. The contribution of the rotation of the oblate core is assumed to be small.

Total Routhian surface (TRS) calculations [32,33] were used to predict the equilibrium deformation in $^{197}$Bi for a proton in the $(\pi, \alpha) = (+, +1/2)$ configuration. Several minima were observed in the potential energy surfaces. The total energy at $\hbar\omega = 0.282$ MeV is plotted in fig. 6 and the obtained minima are listed in table 2. The minimum corresponding to the $\pi[i_{13/2}h^2_{9/2}]_{K=14.5}$ configuration can be identified as the one that has a proton angular momentum of $\sim 14.5\hbar$ along the non-collective oblate axis at $\gamma \sim +60°$. This minimum is associated with a quadrupole deformation of $\beta_2 \sim 0.17$ as seen in table 2 and persists for frequencies between 0.243 and 0.321 MeV.

(At higher frequencies due to the excitation of more quasiparticles, the quadrupole deformation increases rapidly up to 0.27 at $\hbar\omega = 0.555$ MeV.) Since the deformation of the shears band is not expected to differ much from the deformation of the corresponding high-$K$ isomer [22] it seems the shears band in $^{197}$Bi may correspond to moderate oblate deformation.

It has been previously suggested (based on a rotor-plus-particle model calculations) that the contribution of the shears mechanism is greater than that of the rotating oblate core only for small quadrupole deformation of $\varepsilon_2 \leq 0.12$ [19]. Thus, the possibility that a larger quadrupole deformation may be associated with a shears band in the Pb-Bi region requires further investigations.

## 5 Summary

High-spin states were studied in $^{197}$Bi, using the $^{181}$Ta($^{22}$Ne, $6n$) reaction at a beam energy of 125 MeV and the AFRODITE $\gamma$-ray array at iThemba LABS, near Cape Town. The known level scheme of $^{197}$Bi was extended to high spins and a new shears band was found. Its dynamic moment of inertia is larger than that of the known shears bands in the Pb region, and it is likely to indicate the involvement of a third high-$K$ proton intruder orbital. The TRS calculations suggest a quadrupole deformation of $\beta_2 = 0.17$ for a three high-$K$ proton configuration, which is larger than the deformation expected for a shears band in this mass region. More theoretical and experimental studies are needed in order to confirm the proposed high-$K$ proton configuration and to further investigate the deformation associated with this band.

G.K.M. would like to thank iThemba LABS and NRF for the financial assistance throughout the duration of the project.

## References

1. Amita, Ashok Kumar Jain, Balraj Singh, At. Data Nucl. Data Tables **74**, 283 (2000).
2. N. Fotiades *et al.*, Phys. Rev. C **57**, 1624 (1998).
3. A.J.M. Plompen *et al.*, Nucl. Phys. A **562**, 61 (1993).
4. L. Ducroux *et al.*, Z. Phys. A **356**, 241 (1996).
5. M. Kaci *et al.*, Nucl. Phys. A **697**, 3 (2002).
6. M. Kaci *et al.*, Z. Phys. A **354**, 267 (1996).
7. A.K. Singh *et al.*, Nucl. Phys. A **707**, 3 (2002).
8. A. Görgen *et al.*, Nucl. Phys. A **683**, 108 (2001).
9. G. Baldsiefen *et al.*, Nucl. Phys. A **574**, 521 (1994).
10. G. Baldsiefen *et al.*, Nucl. Phys. A **592**, 365 (1995).
11. G. Zwartz *et al.*, J. Phys. G **26**, 849 (2000).
12. P.J. Dagnall *et al.*, J. Phys. G **20**, 1591 (1994).
13. R.M. Clark *et al.*, J. Phys. G **19**, L57 (1993).
14. A.N. Wilson *et al.*, Phys. Lett. B **505**, 6 (2001).
15. S. Frauendorf, Nucl. Phys. A **557**, 259c (1993).
16. S. Frauendorf, Z. Phys. A **358**, 163 (1997).
17. A.O. Macchiavelli *et al.*, Phys. Rev. C **57**, R1073 (1998).
18. A.O. Macchiavelli *et al.*, Phys. Rev. C **58**, R621 (1998).
19. A.O. Macchiavelli *et al.*, Phys. Lett. B **450**, 1 (1999).
20. K. Vyvey *et al.*, Phys. Rev. C **65**, 024320 (2002).
21. K. Vyvey *et al.*, Phys. Rev. Lett. **88**, 102502 (2002).
22. H. Hübel, Prog. Part. Nucl. Phys. **54**, 1 (2005).
23. D.L. Balabanski *et al.*, Eur. Phys. J. A **20**, 191 (2004).
24. T. Chapuran *et al.*, Phys. Rev. C **33**, 130 (1986).
25. X.H. Zhou *et al.*, Z. Phys. A **353**, 3 (1995).
26. R.T. Newman *et al.*, *Proceedings of the Balkan School on Nuclear Physics*, Balkan Phys. Lett., Special Issue, 182 (1998).
27. A. Gavron, Phys. Rev. C **21**, 230 (1980).
28. A. Gavron, *Computational Nuclear Physics 2, Nuclear Reactions* (Springer-Verlag, New York, 1993).
29. D.C. Radford, Nucl. Instrum. Methods Phys. Res. A **361**, 297 (1995).
30. K.S. Krane *et al.*, Nucl. Data Tables **11**, 351 (1973).
31. E. Gueorguieva *et al.*, Nucl. Instrum. Methods Phys. Res. A **474**, 132 (2001).
32. W. Nazarewicz, G.A. Leander, J. Dudek, Nucl. Phys. A **467**, 437 (1987)
33. R. Wyss, W. Satula, W. Nazarewicz, A. Johnson, Nucl. Phys. A **511**, 324 (1990)